Title

Complement factor C1q mediates sleep spindle loss and epileptic spikes after mild brain injury

Journal

Science, 373(6560)

ISSN

0036-8075

Authors

Holden, Stephanie S
Grandi, Fiorella C
Aboubakr, Oumaima
et al.

Publication Date

2021-09-10

DOI

10.1126/science.abj2685

Peer reviewed

HHS Public Access

Author manuscript

Science. Author manuscript; available in PMC 2022 January 11.

Published in final edited form as:

Science. 2021 September 10; 373(6560): eabj2685. doi:10.1126/science.abj2685.

Complement factor C1q mediates sleep spindle loss and epileptic spikes after mild brain injury

Stephanie S Holden[1,2,3], **Fiorella C Grandi**[2,3], **Oumaima Aboubakr**[2], **Bryan Higashikubo**[2], **Frances S Cho**[1,2,3], **Andrew H Chang**[2], **Alejandro Osorio Forero**[4], **Allison R. Morningstar**[2], **Vidhu Mathur**[5], **Logan J Kuhn**[5], **Poojan Suri**[5], **Sethu Sankaranarayanan**[5], **Yaisa Andrews-Zwilling**[5], **Andrea J. Tenner**[6], **Anita Luthi**[4], **Eleonora Aronica**[7,8], **M. Ryan Corces**[2,3], **Ted Yednock**[5], **Jeanne T Paz**[*,1,2,3,9]

[1]Neurosciences Graduate Program, University of California, San Francisco, San Francisco CA 94158, USA.

[2]Gladstone Institute of Neurological Disease, Gladstone Institutes, San Francisco CA 94158, USA.

[3]Department of Neurology, University of California, San Francisco, San Francisco CA 94158, USA.

[4]Department of Fundamental Neurosciences, University of Lausanne, Lausanne, Switzerland.

[5]Annexon Biosciences, South San Francisco CA 94080, USA.

[6]Department of Molecular Biology and Biochemistry, University of California, Irvine, CA 92697, USA.

[7]Department of Neuropathology, Amsterdam UMC, University of Amsterdam, 1105 AZ, Amsterdam, The Netherlands.

[8]Stichting Epilepsie Instellingen Nederland (SEIN), Heemstede, The Netherlands.

[9]The Kavli Institute for Fundamental Neuroscience, and The Weill Institute for Neurosciences, University of California San Francisco, San Francisco CA 94158, USA.

Abstract

Although traumatic brain injury (TBI) acutely disrupts the cortex, most TBI-related disabilities reflect secondary injuries that accrue over time. The thalamus is a likely site of secondary damage because of its reciprocal connections with the cortex. Using a mouse model of mild

[*]Corresponding author. jeanne.paz@gladstone.ucsf.edu.

Author contributions: Conceptualization: JTP and SSH; Data curation: SSH, JTP, FSC, EA, FCG, MRC; Formal analysis: SSH, FSC, FCG, MRC, JTP; Funding acquisition: JTP; Investigation: JTP, SSH, FCG, OA, BH, FSC, AHC, AM, VM, LJK, PS, SS, YAZ, EA, MRC; Methodology: JTP, SSH, FCG, BH, SS, MRC, AOF, AL; Project administration: JTP; Resources: JTP, MRC, TY; Supervision: JTP, MRC, AL, YAZ, TY; Visualization: SSH, FCG, OA, MRC, JTP; Writing-original draft: JTP and SSH; Writing – review and editing: all authors.

Competing interests: VM, LJK, PS, SS, YAZ, and TY are employees of Annexon Inc., a venture-funded private biotechnology company. Other authors have no competing interests.

Data and materials availability: Raw and processed data is deposited on GEO under accession number GSE179541. All data are available in the manuscript or the supplementary materials. The anti-C1q antibody was obtained under a Material Agreement with Annexon.

TBI (mTBI), we found a chronic increase in C1q expression specifically in the corticothalamic system. Increased C1q expression colocalized with neuron loss and chronic inflammation and correlated with disruption in sleep spindles and emergence of epileptic activities. Blocking C1q counteracted these outcomes, suggesting that C1q is a disease modifier in mTBI. Single-nucleus RNA sequencing demonstrated that microglia are a source of thalamic C1q. The corticothalamic circuit could thus be a new target for treating TBI-related disabilities.

One sentence summary

The complement factor C1q mediates loss of local sleep spindles and emergence of epileptic spikes after mild TBI.

Traumatic brain injury (TBI) is a leading cause of disability in children and adults (1). TBI affects 69 million people worldwide yearly (2) and can lead to cognitive dysfunction, difficulty with sensory processing, sleep disruption, and epilepsy. Most of these adverse outcomes manifest months or years after TBI and are caused by indirect secondary injuries that develop as consequences of the initial impact (3). Because the primary injury is essentially irreversible, understanding where, when, and how secondary injuries develop is crucial for preventing or treating disability following TBI.

The cortex is often the site of primary injury because it sits directly beneath the skull. However, the cortex belongs to many larger circuits, in particular the cortico-thalamo-cortical loop. This circuit is important for sensory processing, attention, cognition, and sleep (3–5). The thalamus itself, although not acutely injured in TBI, experiences secondary injury, presumably because of its long-range reciprocal connections with the cerebral cortex (6–10). Structural changes in the thalamus have been implicated in a number of long-term TBI-related health outcomes (11, 12), and patients with TBI display secondary and chronic neurodegeneration and inflammation in thalamic nuclei (13, 14).

Chronic neuroinflammation is common at secondary injury sites (15), but most attempts to improve post-TBI cognitive outcomes with broad anti-inflammatory agents have failed (15, 16). One potential mediator of post-TBI inflammation and injury is the complement pathway, which is activated in the peri-injury area of brain lesions (17–19). Complement activation contributes to inflammation and neurotoxicity in central nervous system (CNS) injury and is increased in human brains afflicted with injury, epilepsy, and Alzheimer's disease (19–23). Aberrant activation of C1, the initiating molecule of the classical complement cascade, can trigger elimination of synapses and contribute to the progression of neurodegenerative disease (24). Conversely, C1/C1q is involved in normal synapse pruning during development (25) and the complement system plays an important part in brain homeostasis by clearing cellular debris and protecting the CNS from infection (20).

We investigated the role of C1q in post-TBI impairment of the corticothalamic system's function, with particular emphasis on the timing and location of C1q expression. We used a mouse model of mild TBI (mTBI), which does not acutely affect subcortical structures, and monitored neurophysiological changes in various regions of the cortex and thalamus using cellular electrophysiology and wireless cortical recordings in freely behaving mice.

Secondary C1q expression coincides with chronic inflammation, neurodegeneration, and synaptic dysfunction in the thalamus

We induced a mild impact injury to the right primary somatosensory cortex (S1) of adult mice (Fig. 1A) and assessed its impact on the brain 3 weeks later. This period corresponds to the latent phase in humans, when the brain is undergoing adaptive and maladaptive changes after injury (26). We stained coronal brain sections with markers of neurons (NeuN) and of glial inflammation (C1q, classical complement pathway; GFAP, astrocytes; IBA1, microglia/macrophages) (Fig. 1, C to E). Three weeks after surgery, mTBI mice had significantly higher GFAP, C1q, and IBA1 expression in the peri-TBI S1 cortex and the functionally connected ventrobasal thalamus (VB) and reticular thalamic nucleus (nRT) than did sham mice (Fig. 1, B to E). We also saw increased expression of similar inflammatory markers in thalamic tissue from human TBI patients, confirming that thalamic inflammation is a consequence of TBI in humans too (Fig. S1).

Glial inflammation was associated with significant neuronal loss in the thalamic region, particularly in the nRT (Fig. 1D and E, Fig. 2A). The nRT of mTBI mice had significantly fewer neurons than the nRT of sham mice, particularly in the “body” region, which receives most of its excitatory inputs from the injured somatosensory cortex (27–31) (Fig. 2, B to C).

To test whether C1q might mark functional damage in the cortex and thalamus, we performed whole-cell patch-clamp recordings in brain slices obtained 3 to 6 weeks after injury. We recorded layer-5 pyramidal neurons – a layer with neurons known to project to both relay thalamus and nRT (32) – and fast-spiking GABAergic interneurons in the peri-TBI S1 cortex, glutamatergic neurons in the relay VB thalamus, and GABAergic neurons in the nRT. The neurons’ intrinsic membrane electrical properties and the spontaneous excitatory and inhibitory postsynaptic current (sEPSC and sIPSC) properties were similar between sham and mTBI mice in both the peri-TBI cortex and the VB thalamus (Table S1). However, in the nRT, mTBI led to a reduction in the frequency of sIPSCs (Fig. 2, D and E). Furthermore, nRT sEPSCs were smaller in amplitude, and trended toward a lower frequency (Fig. 2, F and G). Immunofluorescence staining for green fluorescent protein in mice expressing Thy1-GcaMP6f, a marker of neuronal calcium levels in corticothalamic neurons, revealed reduced fluorescence in the thalamus after mTBI (Fig. 2, H and I).

We conclude that the major long-term effect of mTBI involves disruption of synaptic transmission in the nRT, which coincides with increased C1q expression, reduced cortical inputs, and local neuronal loss. In contrast, neurons in the peri-TBI cortex and the glutamatergic relay VB thalamus appear normal at chronic stages post-mTBI (Table S1), suggesting that neuronal vulnerability is specific to the GABAergic nRT.

Microglia are a source of C1q in the thalamus

To determine the cellular origin of C1q in the thalamus, we microdissected nRT and VB thalamic tissue three weeks post injury (Fig. 3A) and performed single-nucleus RNA sequencing (snRNA-seq) on 6,228 nuclei from sham mice and 5,220 nuclei from mTBI mice. After correcting for ambient RNA (33) and removing potential doublets (34), or

nuclei with a high percentage of mitochondrial reads, clustering analysis identified the expected cell types, including microglia (*Cx3cr1, P2ry12)*, astrocytes (*Cldn10*, *Fgfr3*), oligodendrocytes (*Mobp, Olig1*), oligodendrocyte progenitors (*Sox8, Pdgfra)*, GABAergic neurons (*Gad1*, *Gad2*), and glutamatergic neurons (*Slc17a6, Slc17a7*), which originated from adjacent thalamocortical relay nuclei (Fig. 3B and fig. S2A). The cellular composition was similar between sham and mTBI samples (Fig. S2, B and C) and we detected a few markers of microglial *(Apoe, Cst3)* and astrocytic *(Apoe, Clu*) activation after mTBI (Fig. S3A).

Microglia expressed high levels of *C1qa*, *C1qb,* and *C1qc*, the three genes that together encode the 18 subunits of C1q (35) (Fig. 3C and fig. S3B). In contrast to our findings at the protein level, the expression of the *C1q* genes in nuclear RNA was not significantly different between mTBI and sham samples (Fig. 3D and fig. S3B). Because this was consistent with previous reports that microglia activation is encoded in cytoplasmic rather than nuclear RNA (36), we examined *C1qa* mRNA in the bulk cytoplasmic fractions of our nuclei preparations using quantitative reverse transcription polymerase chain reaction (qRT-PCR). This analysis showed a trend towards increased *C1qa* mRNA expression after mTBI, in both the thalamus and the cortex (Fig. S3C). Similarly, mature oligodendrocytes and astrocytes in both sham and mTBI mice expressed *C4b,* which acts downstream of C1 in the classical complement pathway (Fig. 3E and fig. S3C). *C4b* expression in nuclear RNA increased 5.2-fold in one subcluster of oligodendrocytes after mTBI (Fig. 3F and fig. S, 3E to G), but did not significantly increase in astrocytes. Cytoplasmic bulk qRT-PCR confirmed a trend towards increased *C4b* and *C2* expression (Fig. S3G) whereas transcripts for other components of the complement pathway, such as *C1ra, C1s1* and *Hc* (C5), were not detected by snRNA-seq or cytoplasmic qRT-PCR (Fig. S3, B and I). These data show that microglia are a source of C1q in the thalamus, although we cannot exclude the possibility that other cell types such as astrocytes and neurons could be additional sources (37–39).

None of the GABAergic neurons showed differential expression of components of the complement pathway between mTBI and sham (Fig. S4). Rather, these neurons upregulated several genes related to mitochondrial function and oxidative phosphorylation, including *Cox6c* and *Cox5a* after mTBI (Fig. S4G and table S2).

Blocking C1q function reduces chronic glial inflammation and neuron loss

Increased C1q expression was chronic (Fig. S5, A and B) and might therefore explain the long-term effects of mTBI. To test this hypothesis, we used an antibody that specifically binds to C1q and blocks its downstream activity (40). Mice were given intraperitoneal. Injections of the C1q antibody or a mouse IgG1 isotype control 24 hours after mTBI or sham surgery, followed by twice-weekly treatments for three weeks.

mTBI mice treated with the anti-C1q antibody showed a strong reduction in inflammation and reduced neuronal loss (Fig. 4, A to C) relative to control-treated mTBI mice, as monitored by immunofluorescent staining. On average they had the same number of nRT neurons as antibody-treated sham mice (Fig. 4C), whereas mTBI mice treated with the control IgG still showed inflammation and neuron loss 3 weeks after mTBI. As an

alternative approach to the antibody treatment, we repeated the study using $C1q^{-/-}$ mice and found that they too exhibited reduced chronic inflammation and a non-significant NeuN loss in the nRT after TBI (Fig. S6).

Measurements of anti-C1q and C1q in the brain and the plasma confirmed that the antibody exerted its effect in the brain rather than peripherally (Fig. S7).

mTBI leads to loss of sleep spindles and increased epileptic spikes which are prevented by anti-C1q treatment

We investigated the impact of mTBI *in vivo* using brain rhythms as a readout of corticothalamic circuit function. We implanted chronic wireless electrocorticographic (ECoG) devices into sham and mTBI mice during the mTBI induction surgery and analyzed changes in ECoG rhythms within a 12-hour window 3 weeks post-surgery. We focused our analysis on sleep spindles, which originate from the nRT during non-rapid-eye-movement sleep in mice (41). Sham mice had similar numbers of sleep spindles in the left and right sensory cortices. In mTBI mice, however, the cortex ipsilateral to injury showed fewer sleep spindles than the contralateral cortex (Fig. 5, A to D). mTBI mice also had focal epileptic spikes ipsilateral to the injury (Fig. 6, A to D).

After 3 weeks of antibody treatment, mTBI mice receiving the anti-C1q antibody had normal numbers of sleep spindles (Fig. 5, B, C, and D), and fewer epileptic spikes than the mTBI mice treated with the isotype control (Fig. 6, B to E).

Discussion

Using electrophysiological approaches at the cellular and circuit levels, we found that mild TBI in mice altered the synaptic properties of nRT neurons specifically and was associated with C1q accumulation. The ensuing sleep disruption and development of epileptic spikes were prevented by blocking the C1q pathway with an antibody that has translational potential.

Previous observations of severe head injury show neurodegeneration in the human nRT (42). Our studies showed that even mild cortical injury can lead to neuronal loss in the nRT three 3 after the injury. The loss of neurons in the nRT could explain some of the synaptic changes we observed in this area. For instance, the reduced frequency of IPSCs 3 weeks after mTBI could reflect a deficit in GABAergic neurons. Loss of GABAergic inhibition in the nRT is known to result in corticothalamic circuit hyperexcitability (*43, 44*), and intra-nRT GABAergic connections are important for coordinating inhibitory output to the excitatory thalamic nuclei and controlling oscillatory thalamic activity (45). We also observed deficits in nRT EPSCs, particularly a lower amplitude, which is consistent with the loss of the excitatory cortical inputs. A similar alteration was found in a mouse model of epilepsy that lacks GluA4 AMPA receptors at the cortico-nRT glutamatergic synapse (46). This defect results in loss of feed-forward inhibition in the thalamus, and epileptic activities (46). We therefore propose that alterations to the nRT EPSCs also contribute to corticothalamic circuit hypersynchrony and seizures.

Unlike nRT neurons, cortical neurons, such as excitatory layer-5 pyramidal neurons and GABAergic fast-spiking interneurons, and the excitatory relay thalamic neurons were not altered by mTBI at chronic time points. These observations suggest the presence of homeostatic mechanisms that reduce chronic hyperexcitability after mTBI in the cortex and relay thalamus. They also confirm that at least certain long-term outcomes of mTBI must result from nRT dysfunction rather than simply from damage to the cortex. Nevertheless, ECoG did reveal some local cortical deficits in sleep spindles and epileptic spikes. The disruption in sleep spindles has been reported in rats and humans with severe TBI (5, 47), and is more frequent in humans with mTBI than in those with severe TBI (48).

Given the emerging role of the nRT in generating local sleep spindles in the cortex (41), we speculate that the local loss of sleep spindles in the cortex results from the secondary damage to the nRT.

C1q has well-documented roles in normal brain function, such as synaptic pruning during development (25), forgetting memories in adulthood (49), and in several neurological disorders, including severe TBI (17–24, 50). We found that even after a mild TBI, C1q expression was highly increased in the thalamus for up to four months after injury. Because our mice with mTBI did not develop chronic generalized tonic-clonic seizures, we could not determine whether blocking C1q could prevent full-blown seizures. However, we observed many other protective effects of the anti-C1q antibody, including reduced inflammation and neurodegeneration and protection against sleep spindle disruption and epileptic spikes. A maladaptive role of C1q, including aberrant synapse loss, has been reported in an *in vivo* mouse model of Alzheimer's disease (22), although other studies have shown that C1q can also play a "beneficial" role in Alzheimer's disease by preventing neurotoxicity caused by amyloid-β (51, 52). C1q's maladaptive role in mTBI may seem paradoxical in light of its beneficial role in neuronal development and adaptive synapse pruning (25, 49). However, there is evidence that different inflammatory types of astrocytes or microglia can be protective or harmful in the brain (53, 54), and this concept could extend to C1q as well. Indeed, C1q levels also increase in the cortex and relay thalamus, but do not appear to have a damaging role at these sites because, unlike in the nRT, their neuronal physiology returns to normal at chronic time points.

Our snRNA-seq results suggest that microglia, rather than the neurons themselves, are a source of C1q, and astrocytes and oligodendrocytes of C4. C4 appears to mediate injury after severe TBI, as shown by reduced motor deficits in $C4^{-/-}$ mice (18), and is a genetic risk factor in schizophrenia in which sleep spindle loss is a major electrophysiological feature (55, 56). Notably, C4 over-expression in mice increases microglia engulfment of synapses (57), which provides a potential mechanism linking C1q/C4 to nRT dysfunction. Thus, activation of C1q/C4 in thalamic glial cells could underlie the nRT vulnerability leading to the transformation of sleep spindles into epileptic spikes. Lack of C5 in our model suggests that nRT dysfunction is not due to C5a-C5aR1 microglial polarization or direct local (nRT) neuronal damage caused by C5a or the membrane attack complex – mechanisms that require C5 expression.

The fact that GABAergic nRT neurons overexpress *Cox6c* and *Cox5a*, which are mitochondrial indicators of disrupted neuronal homeostasis and cell death (58, 59) – 3 weeks after injury indicates that nRT neurons are at least dysfunctional and perhaps still dying at that chronic stage. Because anti-C1q treatment reduces nRT neuronal loss, we speculate that sometime after injury, C1q initiates a cycle of complement activation including C4 production by oligodendrocytes, inflammation and neuronal loss. This cycle adds to the damage presumably caused by the initial loss of cortical input, and maintains the nRT's dysfunctional state, leading to the loss of sleep spindles and a hyperactive thalamic output to the cortex. What makes the nRT uniquely vulnerable to this cycle remains unclear.

In summary, our data point to the complement cascade as a disease modifier that could be targeted after injury (in this study, starting 24 hours later) to avoid the devastating long-term outcomes of mild TBI. This prospect is a possibility becauseanti-C1q treatment is already used in a clinical trial for another neurological disorder (40, 60), and there is an expanding pursuit of complement therapeutics for CNS disorders (61).

Genetic or pharmacological manipulations of the complement pathway can improve the outcomes of severe TBI as well, specifically motor function and memory deficits in mice (17, 18, 62, 63). The complement pathway could therefore become a therapy target for both types of trauma.

Materials and Methods

Animals

All our protocols were approved by the Institutional Animal Care and Use Committee at the University of California, San Francisco and Gladstone Institutes. Precautions were taken to minimize stress and the number of animals used in each set of experiments. Mice were separately housed after surgical implants.

Controlled cortical impact

We anesthetized mice with 2–5% isoflurane and placed them in a stereotaxic frame. We performed a 3 mm craniotomy over the right somatosensory cortex (S1) centered at -1 mm posterior from bregma, +3 mm lateral from the midline. TBI was performed with a CCI device (Impact One Stereotaxic Impactor for CCI, Leica Microsystems) equipped with a metal piston using the following parameters: 3 mm tip diameter, 15° angle, depth 0.8 mm from the dura, velocity 3 m/s, and 100 ms dwell time. Sham animals received identical anesthesia and craniotomy, but the injury was not delivered.

Patch-clamp electrophysiology

Recordings were performed as previously described (31, 46). We visually identified S1, nRT, and VB neurons by differential contrast optics with an Olympus microscope and an infrared video camera. Recording electrodes made of borosilicate glass had a resistance of 2.5–4 MΩ when filled with intracellular solution. Access resistance was monitored in all the recordings, and cells were included for analysis only if the access resistance was <25 MΩ. Intrinsic and bursting properties and sEPSCs were recorded in the presence of picrotoxin (50

μM, Sigma-Aldrich), and the internal solution contained 120 mM potassium gluconate, 11 mM EGTA, 11 mM KCl, 10 mM HEPES, 1 mM $CaCl_2$, and 1 mM $MgCl_2$, pH adjusted to 7.4 with KOH (290 mOsm). We corrected the potentials for -15 mV liquid junction potential.

sIPSCs) were recorded in the presence of kynurenic acid (2 mM, Sigma-Aldrich), and the internal solution contained 135 mM CsCl, 10 mM EGTA, 10 mM HEPES, 5 mM Qx-314 (lidocaine N-ethyl bromide), and 2 mM $MgCl_2$, pH adjusted to 7.3 with CsOH (290 mOsm).

snRNA library construction and sequencing

SnRNA-seq libraries were processed using the Chromium Next GEM Single Cell 3'v3 library kit with dual indexing (10x Genomics) according to the manufacturer's specifications. For every sample, nuclei were diluted to 1,000 nuclei/μl in nuclei dilution buffer, and 9,900 nuclei were loaded onto the Chromium, with a targeted recovery of 6,000 nuclei. Replicate 1 and 2 nuclei were processed on different Chromium runs. Libraries were pooled based on their molar concentrations and sequenced on an Illumina NovaSeq 6000 system using an S1 flow cell and a v1 300-cycle Reagent Kit with 28 cycles for read 1, 90 cycles for read 2, 10 cycles for index i7 and 10 cycles for index i5. Cell Ranger (4.0.0) (10x Genomics) was used to perform sample de-multiplexing, barcode processing and single-nucleus gene-UMI counting. Reads were mapped to mm10 (GENCODE vM23/ Ensembl 98, from 10x). From replicate 1, we recovered 2,337 nuclei from sham mice with a mean of 92,533 reads per nucleus, and 650 nuclei from mTBI mice with a mean of 162,363 reads per nuclei; from Replicate 2, we recovered 3,891 nuclei from sham mice with a mean of 47,592 reads per nucleus, and 4,575 nuclei from TBI mice with a mean of 41,658 reads per nucleus. Across all samples and replicates the median number of genes per nucleus was 2,200. Additional detailed are described in supplementary materials and methods.

Statistical analyses

All numerical values are given as means and error bars are standard error of the mean (SEM) unless stated otherwise. Parametric and non-parametric tests were chosen as appropriate and were reported in figure legends. Data analysis was performed with MATLAB (SCR_001622), GraphPad Prism 7/8 (SCR_002798), ImageJ (SCR_003070), Ponemah/NeuroScore (SCR_017107), pClamp (SCR_011323), and Spike2 (SCR_000903) software.

Analysis of electrophysiological properties

The input resistance (R_{in}) and membrane time constant (τ_m) were measured from the membrane hyperpolarization in response to low intensity current steps (-20 to -60 pA). The reported rheobase averages and SEMs were calculated on the basis of the current which first caused at least one action potential during the stimulus per recording. All data from Table S1 were analyzed using a Mann-Whitney test with $\alpha = 0.05$ (*$p < 0.05$, **$p < 0.01$, ***$p < 0.001$, ****$p < 0.0001$), using GraphPad Prism 7 (SCR_002798).

Cumulative probability distributions were generated in MATLAB (SCR_001622) from 11 sham nRT neurons and nine TBI neurons, using 200 randomly selected events from each cell.

Spindle and epileptic spike event detection in ECoG

Data analysis was performed using Spike2 (version 7.20, Cambridge Electronic Design, Cambridge, UK) and Python 3.7 (Python Software Foundation). Epochs were assigned as NREM sleep if the ratio of delta (δ, 1.5 – 4 Hz) to total power (1.5 – 80 Hz) for ECoG was higher than the threshold value with no locomotor activity. Sleep spindle analysis was performed for a period of 12 hours (7 am – 7 pm) at day 20 or 21 after mTBI/sham surgery. Epileptic spikes were analyzed during the same time frame. Recordings were not analyzed during locomotion because it was challenging to reliably distinguish movement artifacts from epileptic spikes (Fig. 6).

We used the Morlet Wavelet function to detect spindles in the 8–15 Hz frequency range. We applied a threshold of [1 x the mean + 1.5 x the S.D.] of the ECoG power, and detected all events above this threshold that lasted at least 0.5 seconds (Fig. 5, Fig. S8). All detected events were visually validated by a scientist blinded to the groups. The onset and offset times of a spindle event were extended to the closest cycle at 0 crossing before and after the threshold. Amplitudes of spindles were computed from the average amplitude of the spindle (8–15Hz) power between onset and offset time, divided by root mean square of the raw ECoG signal, and averaged per mouse. False positive events that contained epileptic spikes (defined as events that exceeded the threshold of 1 x the mean of the baseline + 7 x S.D., Figs. 5–6) were rejected after visual inspection of a scientist blinded to the groups.

Anti-C1q antibody treatment

Anti-C1q antibody (ANX-M1, Annexon Biosciences) (22, 40, 64) and control (mouse isotype IgG1 antibody, MOPC, Clone BE0083, from BioXCell) were administered at 100 mg/kg, a non-toxic dose in rodents, first 24 hours post-TBI, and then every three days for three weeks. Detailed treatment paradigm and pharmacological assays are described in Supplementary Methods.

Supplementary Material

Refer to Web version on PubMed Central for supplementary material.

Acknowledgements:

Thanks to Ben Barres for his inspiration and scientific guidance at the early stage of this project. Thanks to Jasper Anink for help with histology on human tissue, Irene Lew for mouse colony management, Françoise Chanut for editorial support, and Meredith Calvert and the Gladstone Histology & Light Microscopy Core for help with confocal microscopy and ROI analysis. Sequencing was performed at the Center for Advanced Technology (CAT) at UCSF.

Funding:

This study was funded mainly by DoD EP150038 grant to JTP, who also had support from R01 NS078118, NSF 1608236, Gladstone Institutes, the Michael Prize, the Vilcek Prize, and the Kavli Institute for Fundamental Neuroscience. SSH was supported by the Achievement Rewards for College Scientists Scholarship, the Ford

Foundation Dissertation Fellowship, NIH grant T32-GM007449, and the Weill Foundation; BH by the American Epilepsy Society Postdoctoral Research Fellowship; FSC by NINDS F31 NS111819–01A1, the NSF Graduate Research Fellowship #1144247, and the UCSF Discovery Fellowship; EA by Epilepsiefonds project 2020–02; AL by the Swiss National Science Foundation (n° 310030–184759); AOF was supported by the Faculty of Biology and Medicine-University of Lausanne doctoral Fellowship; AJT by NIH R01AG060148.

References and notes

1. World Health Organization, Ed., Neurological disorders: public health challenges (World Health Organization, Geneva, 2006).
2. Dewan MC, Rattani A, Gupta S, Baticulon RE, Hung Y-C, Punchak M, Agrawal A, Adeleye AO, Shrime MG, Rubiano AM, Rosenfeld JV, Park KB, Estimating the global incidence of traumatic brain injury. J Neurosurg, 1–18 (2018).
3. Mckee AC, Daneshvar DH, The neuropathology of traumatic brain injury. Handb Clin Neurol 127, 45–66 (2015). [PubMed: 25702209]
4. Briggs F, Usrey WM, Emerging views of corticothalamic function. Curr Opin Neurobiol 18, 403–407 (2008). [PubMed: 18805486]
5. Sandsmark DK, Elliott JE, Lim MM, Sleep-Wake Disturbances After Traumatic Brain Injury: Synthesis of Human and Animal Studies. Sleep 40 (2017), doi:10.1093/sleep/zsx044.
6. Auladell C, Pérez-Sust P, Supèr H, Soriano E, The early development of thalamocortical and corticothalamic projections in the mouse. Anat Embryol (Berl) 201, 169–179 (2000). [PubMed: 10664178]
7. Blakemore C, Molnar Z, Factors Involved in the Establishment of Specific Interconnections between Thalamus and Cerebral Cortex. Cold Spring Harb Symp Quant Biol 55, 491–504 (1990). [PubMed: 2132833]
8. Antón-Bolaños N, Espinosa A, López-Bendito G, Developmental interactions between thalamus and cortex: a true love reciprocal story. Curr Opin Neurobiol 52, 33–41 (2018). [PubMed: 29704748]
9. Beenhakker MP, Huguenard JR, Neurons that fire together also conspire together: is normal sleep circuitry hijacked to generate epilepsy? Neuron 62, 612–632 (2009). [PubMed: 19524522]
10. Paz JT, Huguenard JR, Microcircuits and their interactions in epilepsy: is the focus out of focus? Nat Neurosci 18, 351–359 (2015). [PubMed: 25710837]
11. Grossman EJ, Ge Y, Jensen JH, Babb JS, Miles L, Reaume J, Silver JM, Grossman RI, Inglese M, Thalamus and cognitive impairment in mild traumatic brain injury: a diffusional kurtosis imaging study. J Neurotrauma 29, 2318–2327 (2012). [PubMed: 21639753]
12. Grossman EJ, Inglese M, The Role of Thalamic Damage in Mild Traumatic Brain Injury. J Neurotrauma 33, 163–167 (2016). [PubMed: 26054745]
13. Ross DT, Ebner FF, Thalamic retrograde degeneration following cortical injury: an excitotoxic process? Neuroscience 35, 525–550 (1990). [PubMed: 2166245]
14. Scott G, Hellyer PJ, Ramlackhansingh AF, Brooks DJ, Matthews PM, Sharp DJ, Thalamic inflammation after brain trauma is associated with thalamo-cortical white matter damage. J Neuroinflammation 12, 224 (2015). [PubMed: 26627199]
15. Simon DW, McGeachy MJ, Bayır H, Clark RSB, Loane DJ, Kochanek PM, The far-reaching scope of neuroinflammation after traumatic brain injury. Nat Rev Neurol 13, 171–191 (2017). [PubMed: 28186177]
16. Russo MV, McGavern DB, Inflammatory neuroprotection following traumatic brain injury. Science 353, 783–785 (2016). [PubMed: 27540166]
17. Krukowski K, Chou A, Feng X, Tiret B, Paladini M-S, Riparip L-K, Chaumeil MM, Lemere C, Rosi S, Traumatic Brain Injury in Aged Mice Induces Chronic Microglia Activation, Synapse Loss, and Complement-Dependent Memory Deficits. Int J Mol Sci 19 (2018), doi:10.3390/ijms19123753.
18. You Z, Yang J, Takahashi K, Yager PH, Kim H-H, Qin T, Stahl GL, Ezekowitz RAB, Carroll MC, Whalen MJ, Reduced Tissue Damage and Improved Recovery of Motor Function after Traumatic Brain Injury in Mice Deficient in Complement Component C4. J Cereb Blood Flow Metab 27, 1954–1964 (2007). [PubMed: 17457366]

19. Bellander B-M, Singhrao SK, Ohlsson M, Mattsson P, Svensson M, Complement Activation in the Human Brain after Traumatic Head Injury. Journal of Neurotrauma 18, 1295–1311 (2001). [PubMed: 11780861]

20. Hammad A, Westacott L, Zaben M, The role of the complement system in traumatic brain injury: a review. J Neuroinflammation 15 (2018), doi:10.1186/s12974-018-1066-z.

21. Wyatt SK, Witt T, Barbaro NM, Cohen-Gadol AA, Brewster AL, Enhanced classical complement pathway activation and altered phagocytosis signaling molecules in human epilepsy. Exp Neurol 295, 184–193 (2017). [PubMed: 28601603]

22. Hong S, Beja-Glasser VF, Nfonoyim BM, Frouin A, Li S, Ramakrishnan S, Merry KM, Shi Q, Rosenthal A, Barres BA, Lemere CA, Selkoe DJ, Stevens B, Complement and Microglia Mediate Early Synapse Loss in Alzheimer Mouse Models. Science 352, 712–716 (2016). [PubMed: 27033548]

23. Lui H, Zhang J, Makinson SR, Cahill MK, Kelley KW, Huang H-Y, Shang Y, Oldham MC, Martens LH, Gao F, Coppola G, Sloan SA, Hsieh CL, Kim CC, Bigio EH, Weintraub S, Mesulam M-M, Rademakers R, Mackenzie IR, Seeley WW, Karydas A, Miller BL, Borroni B, Ghidoni R, Farese RV, Paz JT, Barres BA, Huang EJ, Progranulin Deficiency Promotes Circuit-Specific Synaptic Pruning by Microglia via Complement Activation. Cell 165, 921–935 (2016). [PubMed: 27114033]

24. Cho K, Emerging Roles of Complement Protein C1q in Neurodegeneration. Aging Dis 10, 652–663 (2019). [PubMed: 31165008]

25. Stevens B, Allen NJ, Vazquez LE, Howell GR, Christopherson KS, Nouri N, Micheva KD, Mehalow AK, Huberman AD, Stafford B, Sher A, Litke AM, Lambris JD, Smith SJ, John SWM, Barres BA, The classical complement cascade mediates CNS synapse elimination. Cell 131, 1164–1178 (2007). [PubMed: 18083105]

26. Ding K, Gupta PK, Diaz-Arrastia R, in Translational Research in Traumatic Brain Injury, Laskowitz D, Grant G, Eds. (CRC Press/Taylor and Francis Group, Boca Raton (FL), 2016; http://www.ncbi.nlm.nih.gov/books/NBK326716/), Frontiers in Neuroscience.

27. Destexhe A, Contreras D, Steriade M, Mechanisms Underlying the Synchronizing Action of Corticothalamic Feedback Through Inhibition of Thalamic Relay Cells. Journal of Neurophysiology 79, 999–1016 (1998). [PubMed: 9463458]

28. Golshani P, Liu XB, Jones EG, Differences in quantal amplitude reflect GluR4- subunit number at corticothalamic synapses on two populations of thalamic neurons. Proc Natl Acad Sci U S A 98, 4172–4177 (2001). [PubMed: 11274440]

29. Bourassa J, Pinault D, Deschênes M, Corticothalamic Projections from the Cortical Barrel Field to the Somatosensory Thalamus in Rats: A Single-fibre Study Using Biocytin as an Anterograde Tracer. European Journal of Neuroscience 7, 19–30 (1995).

30. Lam Y-W, Sherman SM, Functional Organization of the Thalamic Input to the Thalamic Reticular Nucleus. J Neurosci 31, 6791–6799 (2011). [PubMed: 21543609]

31. Clemente-Perez A, Makinson SR, Higashikubo B, Brovarney S, Cho FS, Urry A, Holden SS, Wimer M, Dávid C, Fenno LE, Acsády L, Deisseroth K, Paz JT, Distinct Thalamic Reticular Cell Types Differentially Modulate Normal and Pathological Cortical Rhythms. Cell Rep 19, 2130–2142 (2017). [PubMed: 28591583]

32. Deschênes M, Veinante P, Zhang ZW, The organization of corticothalamic projections: reciprocity versus parity. Brain Res Brain Res Rev 28, 286–308 (1998). [PubMed: 9858751]

33. Young MD, Behjati S, SoupX removes ambient RNA contamination from droplet-based single-cell RNA sequencing data. Gigascience 9, giaa151 (2020).

34. McGinnis CS, Murrow LM, Gartner ZJ, DoubletFinder: Doublet Detection in Single-Cell RNA Sequencing Data Using Artificial Nearest Neighbors. Cell Syst 8, 329–337.e4 (2019). [PubMed: 30954475]

35. Lepow IH, Naff GB, Todd EW, Pensky J, Hinz CF, Chromatographic resolution of the first component of human complement into three activities. J Exp Med 117, 983–1008 (1963). [PubMed: 13929797]

36. Thrupp N, Sala Frigerio C, Wolfs L, Skene NG, Fattorelli N, Poovathingal S, Fourne Y, Matthews PM, Theys T, Mancuso R, de Strooper B, Fiers M, Single-Nucleus RNA-Seq Is Not Suitable

for Detection of Microglial Activation Genes in Humans. Cell Rep 32 (2020), doi:10.1016/j.celrep.2020.108189.

37. Bialas AR, Stevens B, TGF-β signaling regulates neuronal C1q expression and developmental synaptic refinement. Nat Neurosci 16, 1773–1782 (2013). [PubMed: 24162655]
38. Schartz ND, Tenner AJ, The good, the bad, and the opportunities of the complement system in neurodegenerative disease. J Neuroinflammation 17, 354 (2020). [PubMed: 33239010]
39. Wu T, Dejanovic B, Gandham VD, Gogineni A, Edmonds R, Schauer S, Srinivasan K, Huntley MA, Wang Y, Wang T-M, Hedehus M, Barck KH, Stark M, Ngu H, Foreman O, Meilandt WJ, Elstrott J, Chang MC, Hansen DV, Carano RAD, Sheng M, Hanson JE, Complement C3 Is Activated in Human AD Brain and Is Required for Neurodegeneration in Mouse Models of Amyloidosis and Tauopathy. Cell Rep 28, 2111–2123.e6 (2019). [PubMed: 31433986]
40. Lansita JA, Mease KM, Qiu H, Yednock T, Sankaranarayanan S, Kramer S, Nonclinical Development of ANX005: A Humanized Anti-C1q Antibody for Treatment of Autoimmune and Neurodegenerative Diseases. Int J Toxicol 36, 449–462 (2017). [PubMed: 29202623]
41. Fernandez LM, Vantomme G, Osorio-Forero A, Cardis R, Béard E, Lüthi A, Thalamic reticular control of local sleep in mouse sensory cortex. Elife 7 (2018), doi:10.7554/eLife.39111.
42. Ross DT, Graham DI, Adams JH, Selective loss of neurons from the thalamic reticular nucleus following severe human head injury. J Neurotrauma 10, 151–165 (1993). [PubMed: 8411218]
43. Huntsman MM, Porcello DM, Homanics GE, DeLorey TM, Huguenard JR, Reciprocal inhibitory connections and network synchrony in the mammalian thalamus. Science 283, 541–543 (1999). [PubMed: 9915702]
44. Sohal VS, Huguenard JR, Inhibitory interconnections control burst pattern and emergent network synchrony in reticular thalamus. J Neurosci 23, 8978–8988 (2003). [PubMed: 14523100]
45. Sohal VS, Huntsman MM, Huguenard JR, Reciprocal inhibitory connections regulate the spatiotemporal properties of intrathalamic oscillations. J Neurosci 20, 1735–1745 (2000). [PubMed: 10684875]
46. Paz JT, Bryant AS, Peng K, Fenno L, Yizhar O, Frankel WN, Deisseroth K, Huguenard JR, A new mode of corticothalamic transmission revealed in the Gria4(-/-) model of absence epilepsy. Nat Neurosci 14, 1167–1173 (2011). [PubMed: 21857658]
47. Andrade P, Nissinen J, Pitkänen A, Generalized Seizures after Experimental Traumatic Brain Injury Occur at the Transition from Slow-Wave to Rapid Eye Movement Sleep. J Neurotrauma 34, 1482–1487 (2017). [PubMed: 27707084]
48. Mahmood O, Rapport LJ, Hanks RA, Fichtenberg NL, Neuropsychological performance and sleep disturbance following traumatic brain injury. J Head Trauma Rehabil 19, 378–390 (2004). [PubMed: 15597029]
49. Wang C, Yue H, Hu Z, Shen Y, Ma J, Li J, Wang X-D, Wang L, Sun B, Shi P, Wang L, Gu Y, Microglia mediate forgetting via complement-dependent synaptic elimination. Science 367, 688–694 (2020). [PubMed: 32029629]
50. Vukojicic A, Delestrée N, Fletcher EV, Pagiazitis JG, Sankaranarayanan S, Yednock TA, Barres BA, Mentis GZ, The Classical Complement Pathway Mediates Microglia-Dependent Remodeling of Spinal Motor Circuits during Development and in SMA. Cell Rep 29, 3087–3100.e7 (2019). [PubMed: 31801075]
51. Benoit ME, Hernandez MX, Dinh ML, Benavente F, Vasquez O, Tenner AJ, C1q-induced LRP1B and GPR6 proteins expressed early in Alzheimer disease mouse models, are essential for the C1q-mediated protection against amyloid-β neurotoxicity. J Biol Chem 288, 654–665 (2013). [PubMed: 23150673]
52. Pisalyaput K, Tenner AJ, Complement component C1q inhibits beta-amyloid- and serum amyloid P-induced neurotoxicity via caspase- and calpain-independent mechanisms. J Neurochem 104, 696–707 (2008). [PubMed: 17986223]
53. Liddelow SA, Guttenplan KA, Clarke LE, Bennett FC, Bohlen CJ, Schirmer L, Bennett ML, Münch AE, Chung W-S, Peterson TC, Wilton DK, Frouin A, Napier BA, Panicker N, Kumar M, Buckwalter MS, Rowitch DH, Dawson VL, Dawson TM, Stevens B, Barres BA, Neurotoxic reactive astrocytes are induced by activated microglia. Nature 541, 481–487 (2017). [PubMed: 28099414]

54. Mills CD, Kincaid K, Alt JM, Heilman MJ, Hill AM, M-1/M-2 macrophages and the Th1/Th2 paradigm. J Immunol 164, 6166–6173 (2000). [PubMed: 10843666]
55. Sekar A, Bialas AR, de Rivera H, Davis A, Hammond TR, Kamitaki N, Tooley K, Presumey J, Baum M, Van Doren V, Genovese G, Rose SA, Handsaker RE, Schizophrenia Working Group of the Psychiatric Genomics Consortium, Daly MJ, Carroll MC, Stevens B, McCarroll SA, Schizophrenia risk from complex variation of complement component 4. Nature 530, 177–183 (2016). [PubMed: 26814963]
56. Manoach DS, Pan JQ, Purcell SM, Stickgold R, Reduced Sleep Spindles in Schizophrenia: A Treatable Endophenotype That Links Risk Genes to Impaired Cognition? Biol Psychiatry 80, 599–608 (2016). [PubMed: 26602589]
57. Yilmaz M, Yalcin E, Presumey J, Aw E, Ma M, Whelan CW, Stevens B, McCarroll SA, Carroll MC, Overexpression of schizophrenia susceptibility factor human complement C4A promotes excessive synaptic loss and behavioral changes in mice. Nat Neurosci 24, 214–224 (2021). [PubMed: 33353966]
58. Harris L. k., Black R. t., Golden K. m., Reeves T. m., Povlishock J. t., Phillips L. l., Traumatic Brain Injury-Induced Changes in Gene Expression and Functional Activity of Mitochondrial Cytochrome C Oxidase. Journal of Neurotrauma 18, 993–1009 (2001). [PubMed: 11686499]
59. Opii WO, Nukala VN, Sultana R, Pandya JD, Day KM, Merchant ML, Klein JB, Sullivan PG, Butterfield DA, Proteomic Identification of Oxidized Mitochondrial Proteins following Experimental Traumatic Brain Injury. Journal of Neurotrauma 24, 772–789 (2007). [PubMed: 17518533]
60. Annexon Announces Initiation of Phase 2/3 Trial of ANX005 in Patients with Guillain-Barré Syndrome. BioSpace, (available at https://www.biospace.com/article/annexon-announces-initiation-of-phase-2-3-trial-of-anx005-in-patients-with-guillain-barre-syndrome/).
61. Zelek WM, Xie L, Morgan BP, Harris CL, Compendium of current complement therapeutics. Mol Immunol 114, 341–352 (2019). [PubMed: 31446305]
62. Alawieh A, Chalhoub RM, Mallah K, Langley EF, York M, Broome H, Couch C, Adkins D, Tomlinson S, Complement Drives Synaptic Degeneration and Progressive Cognitive Decline in the Chronic Phase after Traumatic Brain Injury. J Neurosci 41, 1830–1843 (2021). [PubMed: 33446516]
63. Mallah K, Couch C, Alshareef M, Borucki D, Yang X, Alawieh A, Tomlinson S, Complement mediates neuroinflammation and cognitive decline at extended chronic time points after traumatic brain injury. acta neuropathol commun 9, 72 (2021). [PubMed: 33879257]
64. McGonigal R, Cunningham ME, Yao D, Barrie JA, Sankaranarayanan S, Fewou SN, Furukawa K, Yednock TA, Willison HJ, C1q-targeted inhibition of the classical complement pathway prevents injury in a novel mouse model of acute motor axonal neuropathy. Acta Neuropathol Commun 4, 23 (2016). [PubMed: 26936605]
65. Aronica E, Boer K, van Vliet EA, Redeker S, Baayen JC, Spliet WGM, van Rijen PC, Troost D, da Silva FHL, Wadman WJ, Gorter JA, Complement activation in experimental and human temporal lobe epilepsy. Neurobiol Dis 26, 497–511 (2007). [PubMed: 17412602]
66. Schiering IAM, de Haan TR, Niermeijer J-MF, Koelman JH, Majoie CBLM, Reneman L, Aronica E, Correlation between clinical and histologic findings in the human neonatal hippocampus after perinatal asphyxia. J Neuropathol Exp Neurol 73, 324–334 (2014). [PubMed: 24607964]
67. Bell JE, Alafuzoff I, Al-Sarraj S, Arzberger T, Bogdanovic N, Budka H, Dexter DT, Falkai P, Ferrer I, Gelpi E, Gentleman SM, Giaccone G, Huitinga I, Ironside JW, Kliioueva N, Kovacs GG, Meyronet D, Palkovits M, Parchi P, Patsouris E, Reynolds R, Riederer P, Roggendorf W, Seilhean D, Schmitt A, Schmitz P, Streichenberger N, Schwalber A, Kretzschmar H, Management of a twenty-first century brain bank: experience in the BrainNet Europe consortium. Acta Neuropathol 115, 497–507 (2008). [PubMed: 18365220]
68. Ritter-Makinson S, Clemente-Perez A, Higashikubo B, Cho FS, Holden SS, Bennett E, Chkhaidze A, Eelkman Rooda OHJ, Cornet M-C, Hoebeek FE, Yamakawa K, Cilio MR, Delord B, Paz JT, Augmented Reticular Thalamic Bursting and Seizures in Scn1a-Dravet Syndrome. Cell Rep 26, 54–64.e6 (2019). [PubMed: 30605686]
69. Thalamic Models of Seizures In Vitro - ScienceDirect, (available at https://www.sciencedirect.com/science/article/pii/B9780128040669000195).

70. Martinez-Garcia RI, Voelcker B, Zaltsman JB, Patrick SL, Stevens TR, Connors BW, Cruikshank SJ, Two dynamically distinct circuits drive inhibition in the sensory thalamus. Nature 583, 813–818 (2020). [PubMed: 32699410]

71. Cruikshank SJ, Urabe H, Nurmikko AV, Connors BW, Pathway-specific feedforward circuits between thalamus and neocortex revealed by selective optical stimulation of axons. Neuron 65, 230–245 (2010). [PubMed: 20152129]

72. Sorokin JM, Davidson TJ, Frechette E, Abramian AM, Deisseroth K, Huguenard JR, Paz JT, Bidirectional Control of Generalized Epilepsy Networks via Rapid Real-Time Switching of Firing Mode. Neuron 93, 194–210 (2017). [PubMed: 27989462]

73. Corces MR, Trevino AE, Hamilton EG, Greenside PG, Sinnott-Armstrong NA, Vesuna S, Satpathy AT, Rubin AJ, Montine KS, Wu B, Kathiria A, Cho SW, Mumbach MR, Carter AC, Kasowski M, Orloff LA, Risca VI, Kundaje A, Khavari PA, Montine TJ, Greenleaf WJ, Chang HY, An improved ATAC-seq protocol reduces background and enables interrogation of frozen tissues. Nat Methods 14, 959–962 (2017). [PubMed: 28846090]

74. Corces R, Isolation of nuclei from frozen tissue for ATAC-seq and other epigenomic assays (2019), doi:10.17504/protocols.io.6t8herw.

75. Stuart T, Butler A, Hoffman P, Hafemeister C, Papalexi E, Mauck WM, Hao Y, Stoeckius M, Smibert P, Satija R, Comprehensive Integration of Single-Cell Data. Cell 177, 1888–1902.e21 (2019). [PubMed: 31178118]

76. Butler A, Hoffman P, Smibert P, Papalexi E, Satija R, Integrating single-cell transcriptomic data across different conditions, technologies, and species. Nat Biotechnol 36, 411–420 (2018). [PubMed: 29608179]

77. Korsunsky I, Millard N, Fan J, Slowikowski K, Zhang F, Wei K, Baglaenko Y, Brenner M, Loh P-R, Raychaudhuri S, Fast, sensitive and accurate integration of single-cell data with Harmony. Nat Methods 16, 1289–1296 (2019). [PubMed: 31740819]

78. van Dijk D, Sharma R, Nainys J, Yim K, Kathail P, Carr A, Burdziak C, Moon KR, Chaffer CL, Pattabiraman D, Bierie B, Mazutis L, Wolf G, Krishnaswamy S, Pe'er D, Recovering gene interactions from single-cell data using data diffusion. Cell 174, 716–729.e27 (2018). [PubMed: 29961576]

79. Li Y, Lopez-Huerta VG, Adiconis X, Levandowski K, Choi S, Simmons SK, Arias-Garcia MA, Guo B, Yao AY, Blosser TR, Wimmer RD, Aida T, Atamian A, Naik T, Sun X, Bi D, Malhotra D, Hession CC, Shema R, Gomes M, Li T, Hwang E, Krol A, Kowalczyk M, Peça J, Pan G, Halassa MM, Levin JZ, Fu Z, Feng G, Distinct subnetworks of the thalamic reticular nucleus. Nature 583, 819–824 (2020). [PubMed: 32699411]

80. Talley EM, Cribbs LL, Lee JH, Daud A, Perez-Reyes E, Bayliss DA, Differential distribution of three members of a gene family encoding low voltage-activated (T-type) calcium channels. J Neurosci 19, 1895–1911 (1999). [PubMed: 10066243]

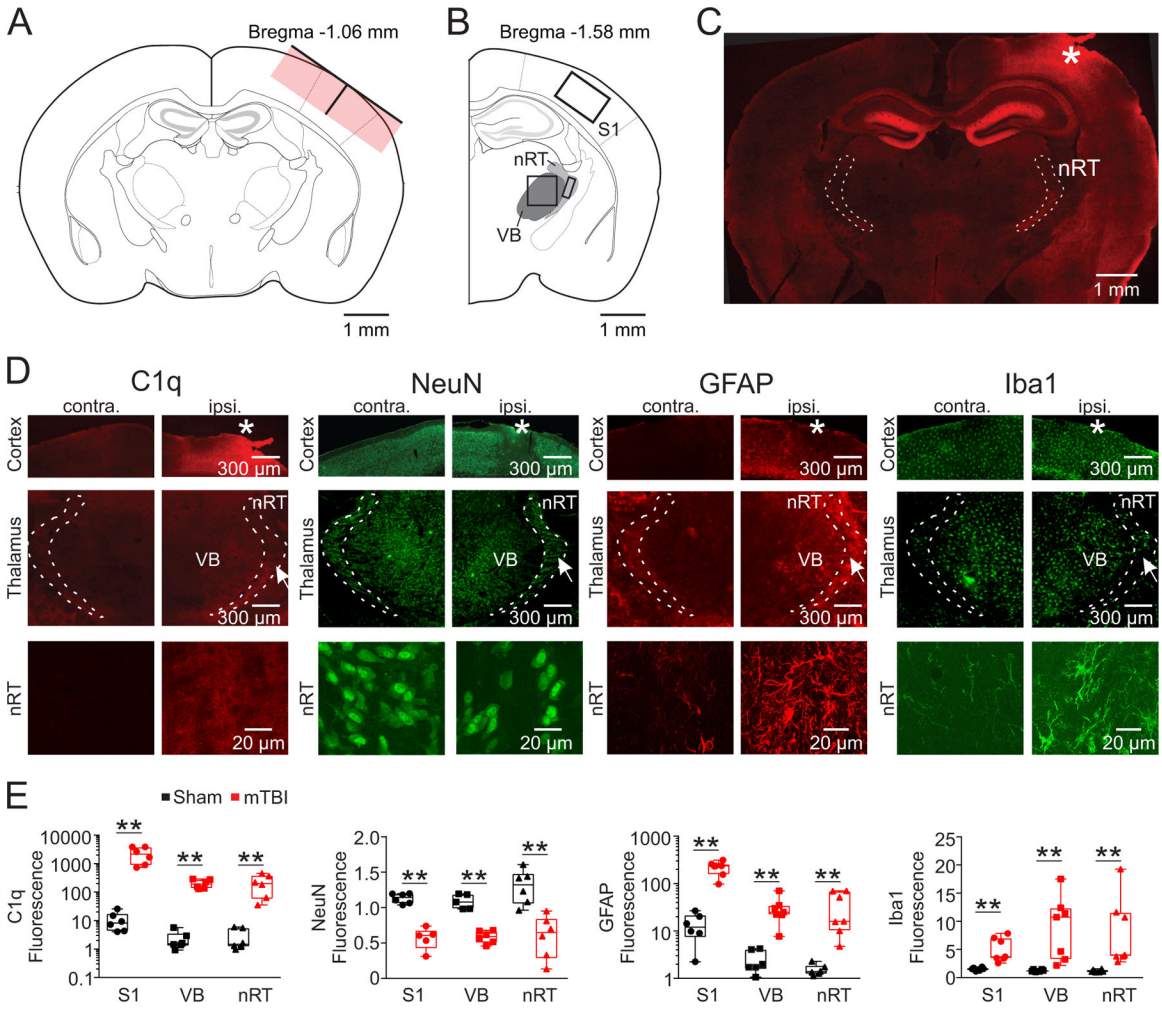

Fig. 1. The injured cortex and functionally connected thalamus show chronic inflammation and neuron loss three weeks after mTBI.

(A, B) Schematic of the controlled cortical impact (A) and of the S1 cortex and nRT and VB thalamic regions (B). **(C)** Coronal brain section from a mTBI mouse stained for C1q. Note that bilateral C1q expression is typical for the hippocampus. **(D)** Close-up images of S1 (top), VB and nRT (middle), and confocal images of nRT (bottom) stained for C1q, NeuN, GFAP, and Iba1. Injury site in the right S1 cortex is marked by an asterisk. Arrow in nRT indicates location of confocal image. **(E)** Fluorescence ratios between ipsilateral and contralateral regions in sham and mTBI mice. Data represent all points from min to max, with a Mann-Whitney test and $\alpha = 0.05$ (*$p < 0.05$, **$p < 0.01$). Analysis includes between five and seven mice per group (n = three sections per mouse, one image per region).

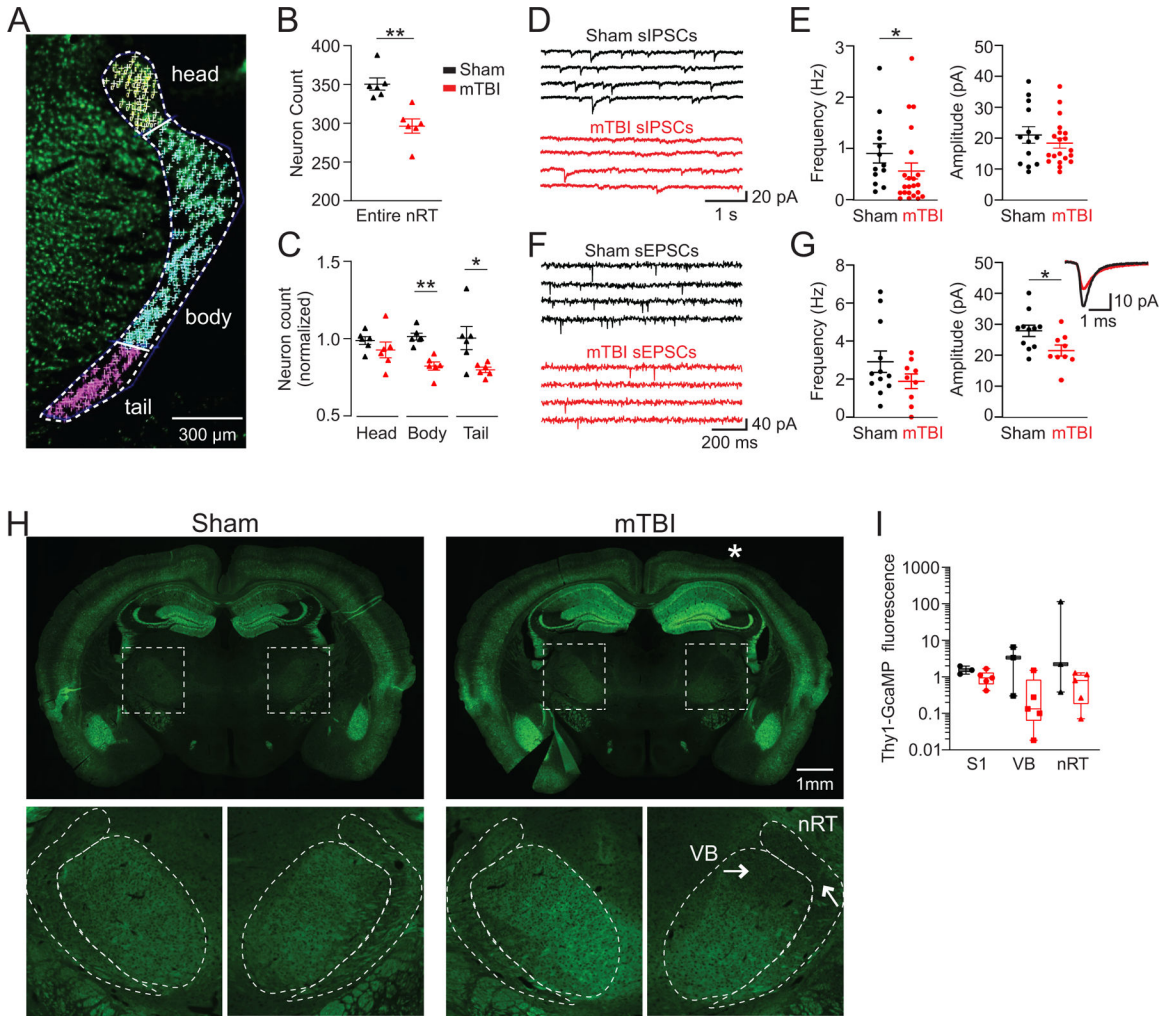

Fig. 2. The nRT ipsilateral to the injured cortex shows neuron loss and altered sIPSC and sEPSC properties three weeks after mTBI.

(A-C) High-magnification coronal image of the nRT (A) and neuron counts across the entire ipsilateral nRT (B) or per subdivision, normalized to the median value from the sham group (C). Six mice per group (n = three sections per mouse, averaged). **(D, E)** sIPSC recordings from nRT (D) neurons and frequency and amplitude distributions (E) in 13 neurons from four sham mice and 22 neurons from six mTBI mice. **(F, G)** Spontaneous EPSC recordings (F) from nRT neurons and frequency and amplitude distributions (G) in 11 neurons from six sham mice and nine neurons from seven mTBI mice. Inset: averaged EPSC traces from single nRT neurons. **(H)** Coronal brain sections from Thy1-GCaMP6f mice with sham surgery and mTBI (asterisk). Bottom: projection terminals from the cortex. **(I)** Thy1-GCaMP fluorescence ratios between ipsilateral and contralateral regions. Data represent all points from min to max, Mean ± SEM, with a Mann-Whitney test and $\alpha = 0.05$ (*$p < 0.05$, **$p < 0.01$). Analysis includes five sham mice and six mTBI mice (n = three sections per mouse, one image per region).

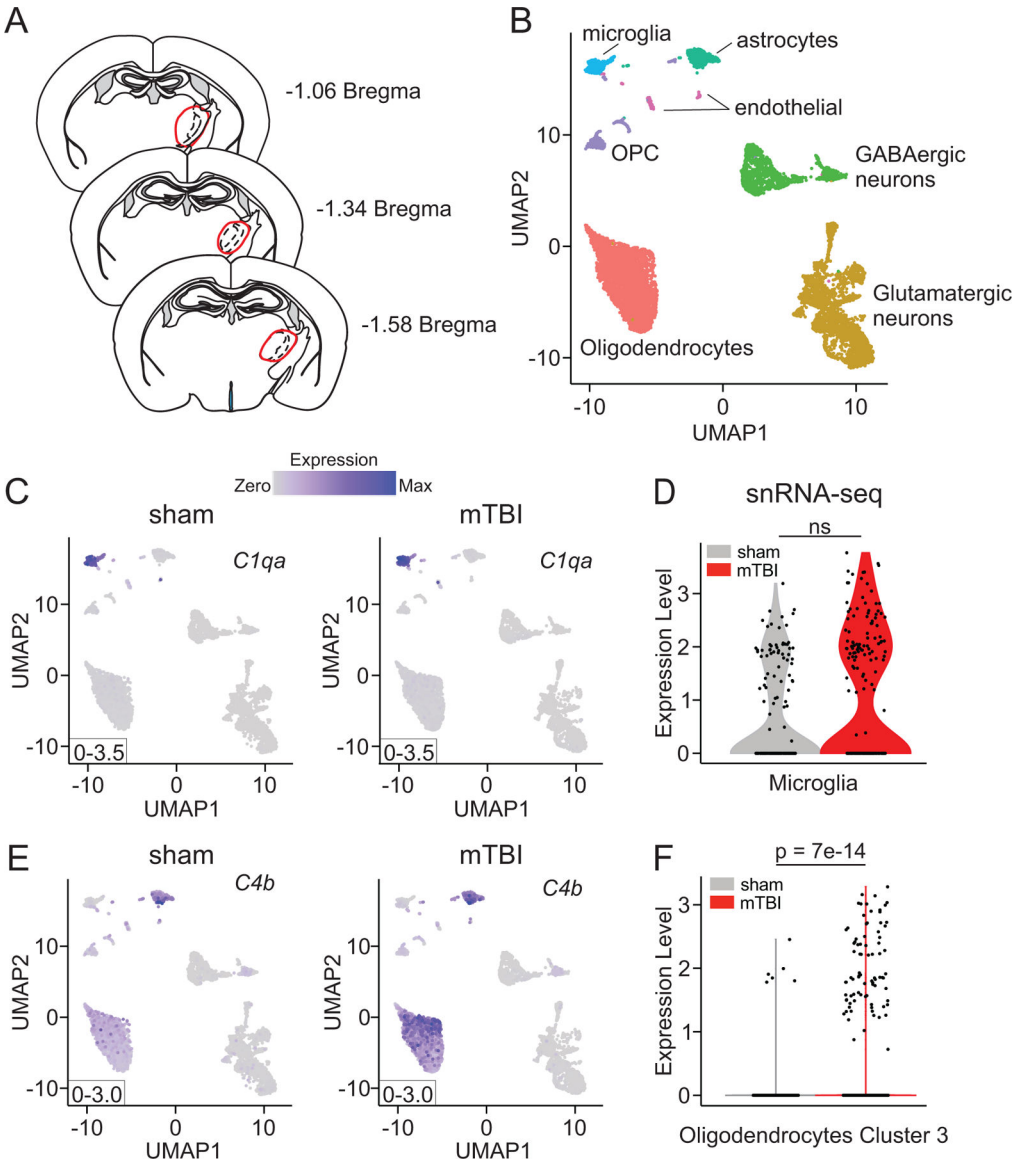

Fig. 3. Microglia are a source of C1q in the thalamus three weeks after mTBI.

(A) Schematic of coronal brain sections showing the location of thalamic tissue dissection. **(B, C, E)** UMAP representation of single-nucleus RNA sequencing data (n = 4,908 sham nuclei, n = 4,338 mTBI nuclei, after data cleaning) colored by cell type or lineage (B), and for nuclear *C1qa* (C) or *C4b* (E) expression. Lineage markers described in Fig. S2A. Normalized expression scale shown above, 0-max, with max value for each panel. **(D, F)** Violin plots of *C1qa* expression in microglial nuclei (D) and of *C4b* expression in oligodendrocyte nuclei (F) from cluster 3 (Oligo 3, Fig. S3E) from sham and mTBI mice, analyzed with a Wilcoxon Rank Sum test (ns = not significant). Analysis combines both technical replicates, collectively representing nine sham mice and ten mTBI mice. Each dot represents a single nucleus.

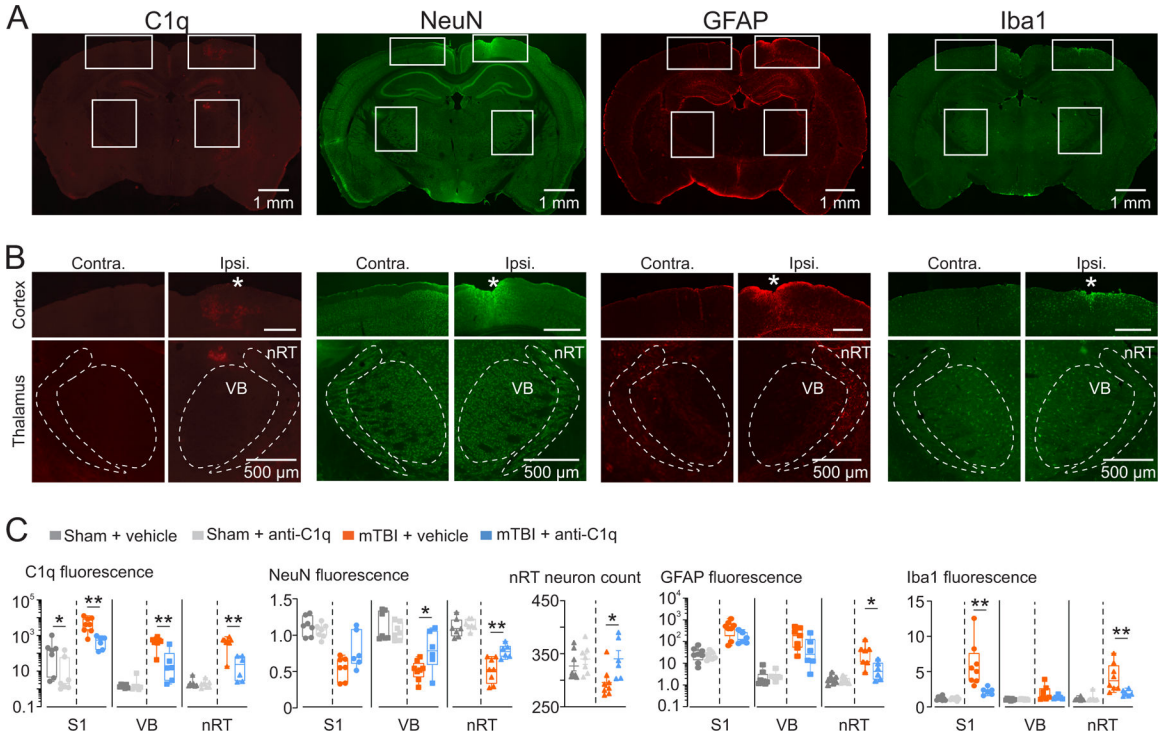

Fig. 4. Anti-C1q antibody reduces chronic inflammation and neuron loss three weeks after mTBI.

(A, B) Coronal brain sections (A) and close-ups (B) of S1 (top), VB and nRT (bottom) from mTBI mice treated with anti-C1q antibody and stained for C1q, NeuN, GFAP, and Iba1. Asterisk marks injury site. **(C)** Quantification of nRT neuron counts and fluorescence ratios between ipsilateral and contralateral regions in sham and mTBI mice treated with the anti-C1q antibody or the isotype control. Data represent all points from min to max, with a Mann-Whitney test and $\alpha = 0.05$ (*$p < 0.05$, **$p < 0.01$). Analysis includes between six and eight mice per group (n = three sections per mouse, one image per region).

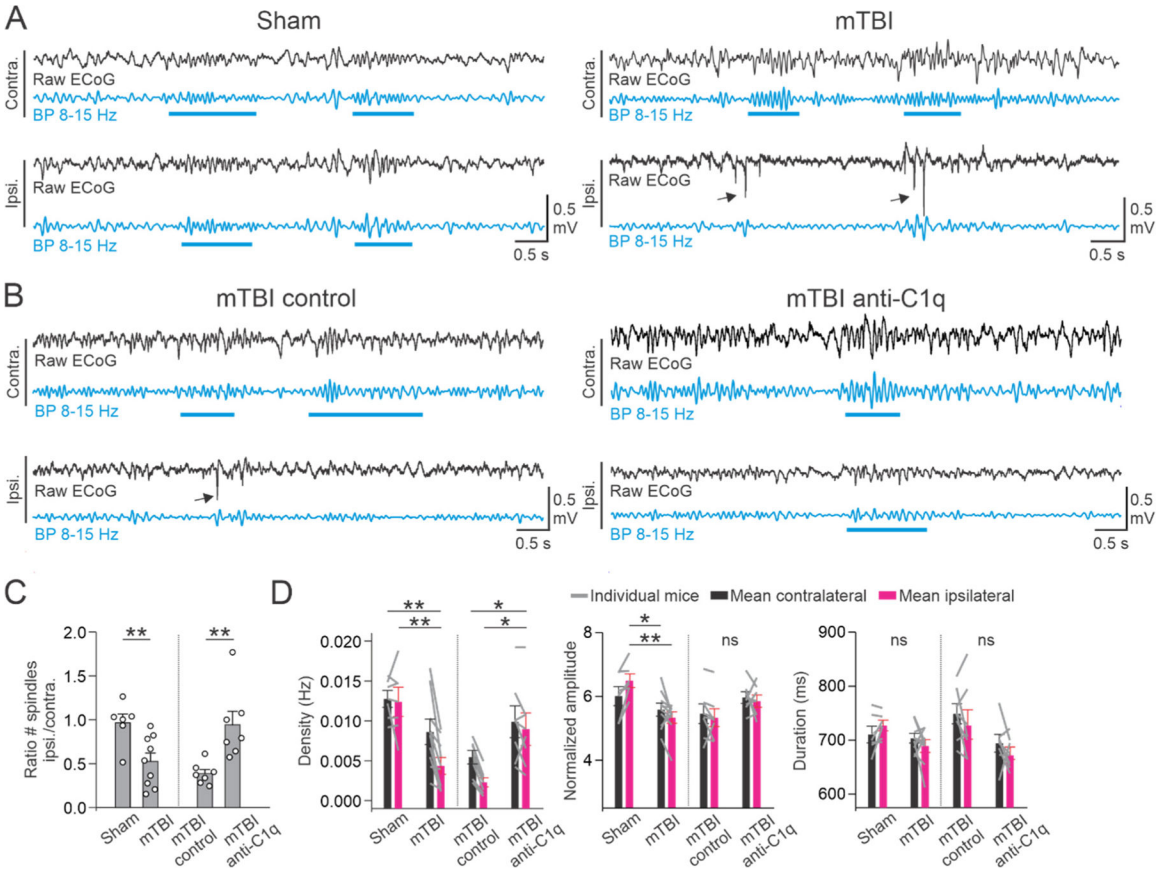

Fig. 5. Anti-C1q antibody reverts chronic sleep spindle reduction after mTBI.

(A) ECoG recordings from a sham and mTBI mouse three weeks after mTBI. Blue traces represent the band-pass (BP, 8—15 Hz) filtered ECoG. Horizontal blue lines show the detected spindles. Arrows indicate epileptic spikes. **(B)** Same as (A) from mTBI mice treated with an isotype control or the anti-C1q antibody. **(C)** Ratio of sleep spindle counts in ipsilateral ECoG to sleep spindle counts in contralateral ECoG detected within a 12-hour window. Data represent mean ± SEM analyzed with a Mann-Whitney rank sum test with $\alpha = 0.05$ (*$p < 0.05$, **$p < 0.01$). Analysis includes n = six sham mice, n = nine mTBI mice (left); n = seven control-treated mTBI mice, n = six antibody-treated mTBI mice (right). **(D)** Density, normalized amplitude and duration of sleep spindles in contralateral and ipsilateral ECoG from the mice in (C). Data represent mean ± SEM analyzed with a Kruskal-Wallis One Way Analysis of Variance on Ranks, all pairwise multiple comparison procedures (Holm-Sidak method), $\alpha = 0.05$ (*$p < 0.05$, **$p < 0.01$). Gray lines connect contralateral and ipsilateral data points for each mouse.

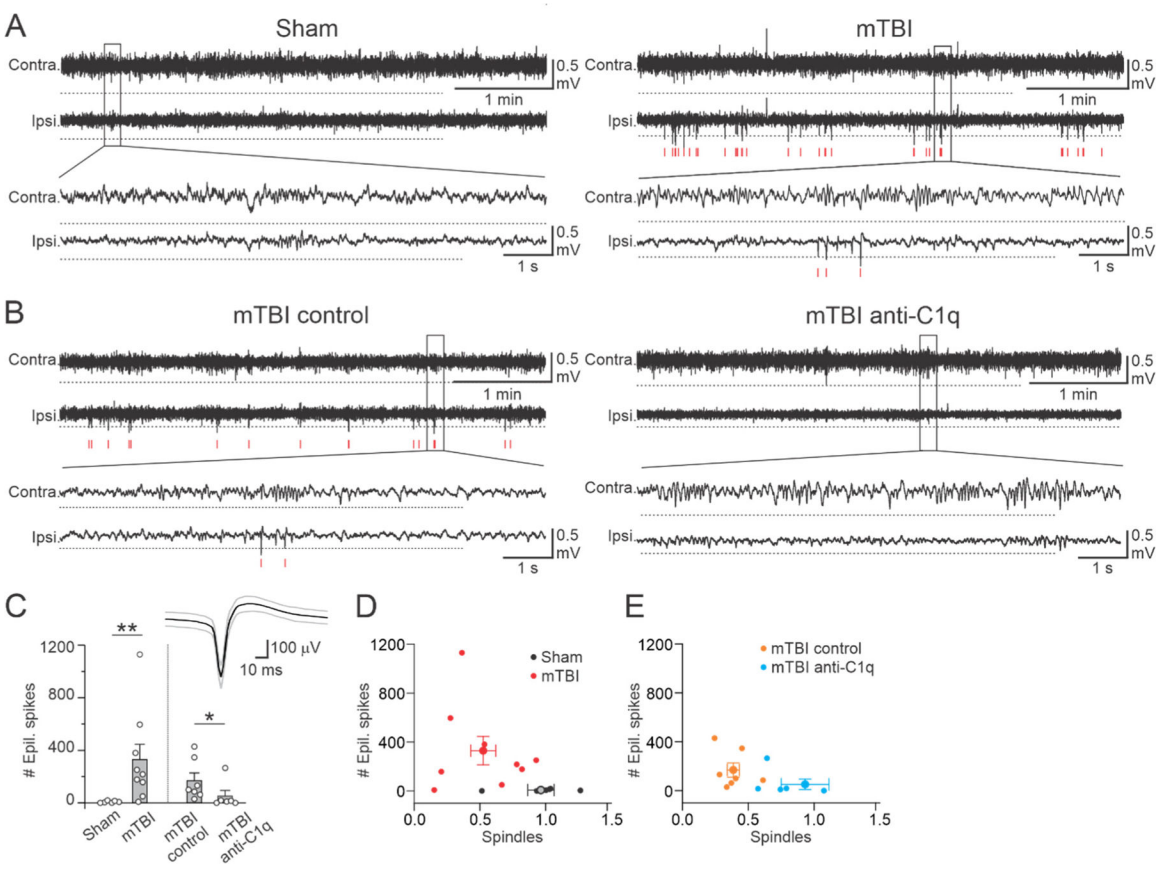

Fig. 6. Anti-C1q antibody reduces focal epileptic spikes that develop three weeks after mTBI.

(A) ECoG recordings from a sham and mTBI mouse three weeks post-mTBI. Horizontal dashed lines represent the spike detection threshold. Vertical red lines indicate detected spikes. **(B)** Same as A) from mTBI mice treated with an isotype control or the anti-C1q antibody. Traces in A-B are from episodes of NREM sleep. **(C)** Number of epileptic spikes detected within a 12-hour window. Data represent mean ± SEM analyzed with a Mann-Whitney rank sum test, $\alpha = 0.05$ (*$p < 0.05$, **$p < 0.01$). Inset: an average epileptic spike from the mTBI mouse shown in (B) (n=592 spikes; mean (black) ± SD (grey). Analysis includes n = six sham mice, n = nine mTBI mice (left); n = seven control-treated mTBI mice, n = six antibody-treated mTBI mice. **(D, E)** Number of epileptic spikes as a function of the ratio of sleep spindles in the sham versus mTBI (D) and anti-C1q versus control mTBI (E) mice from (C). Individual points represent each mouse and error bars represent mean ± SEM across both axes.